The intensity distribution in the Na$_2$ and Li$_2$ A–X bands*

L. K. Lam and A. Gallagher[†]

Joint Institute for Laboratory Astrophysics, National Bureau of Standards and University of Colorado, Boulder, Colorado 80309

M. M. Hessel

Laser Physics Section 277.05, National Bureau of Standards, Boulder, Colorado 80303
(Received 24 November 1976)

The accuracy of the quasistatic or classical Franck–Condon approximation for unresolved bound–bound molecular bands is investigated by comparison with appropriately averaged quantum mechanical calculations. Wavelength-averaged absorption and stimulated emission cross sections are calculated for the A–X bands of Na$_2$ and Li$_2$, representing low resolution or collision broadened spectra, and comparisons are made with experimental spectra. These A–X bands exhibit a red edge, due to a head of heads or a classical satellite, and a comparison of quantum mechanical, classical, and semiclassical satellite shapes is made. The overall quantum mechanical band shapes agree with the classical calculation, except for approximately periodic band structures and nonclassical behavior at the satellites. The emission spectrum resulting from white light or electron excitation of Na$_2$, is also calculated and compared to that observed in an electrical discharge. Finally, emission spectra of Na$_2$ for thermal distributions at various temperatures are compared to the fluorescence spectrum observed from excited dimers formed by an atom–molecule excitation transfer process.

I. INTRODUCTION

The continuous intensity distribution in bound–bound molecular bands is frequently used to estimate molecular potentials and transition moments, and to study collisional processes. When transitions to unbound continuum states contribute to a band, the resulting intensities must also be diagnosed on the basis of continuum band shapes. The intensities in the wings of collisionally broadened atomic lines is included in this topic. In these analyses, the accuracy of the methods used to interpret the continuum intensities normally go untested, because the molecular potentials were not accurately known from bound–bound spectroscopy. The present calculations test the accuracy and limitations of approximate theories frequently used to interpret continuum band intensities, by calculating the exact bound–bound spectrum for known potentials and comparing to the predictions of the models. In order to increase the usefulness of the results and to test the dependence on mass we make these comparisons for the actual cases of the Li$_2$ and Na$_2$ A–X bands. These particular band shapes are of interest for the interpretation of experimental results[1] and diagnostics and modeling of metal vapor lamps[2] and lasers.[3,4] These bands also provide a particularly interesting test case because an extremum occurs in the potential difference between the excited and ground states, causing a "head of heads" or "satellite" at one edge of the band.

The quantum mechanical calculation of a molecular band intensity distribution involves the evaluation of the intensities of all allowed transitions between the vibrational–rotational levels of the upper and lower states. For comparison to observations these lines are then grouped according to their wave numbers and averaged over some suitable bandwidth $\Delta \nu$ corresponding to an experimental resolution or a Doppler plus collisionally broadened linewidth. If the upper and lower states are

both strongly bound and their R_e are similar, the spectrum is predominately due to bound–bound transitions, and the calculation utilizes well established principles for bound-state Franck–Condon factors. The present calculations require the evaluation of about 10^3 Franck–Condon factors and the sorting of $\sim 10^5$ lines for each molecular band. Thus it is desirable to find accurate simplifying approximations. One such approximation, which treats the rotational lines of each vibrational band as a continuum, is evaluated here and found to be very effective.

Band intensity calculations of the present type have rarely been carried out, doubtless due largely to the magnitude of the calculation, particularly for heavy molecules. Calculations have been reported for H$_2$,[5] H$_2^+$,[6] He$_2$,[7,8] CsAr,[9] and Br$_2$.[10] The H$_2$, H$_2^+$, and He$_2$ spectra are highly quantum mechanical due to the light mass of the molecules, while the CsAr case is quite classical due to an initial population distribution that encompasses many vibrational and rotational states. Regular intensity undulations are considered in several of these references, and a satellite of the H$_2$ B–X band is considered in Ref. 8. All of the above calculations are for bound–free, free–bound, or free–free transitions.

Interpretations of continuum band intensities frequently utilize, explicitly or implicitly, the classical Franck–Condon principle (CFCP) or the equivalent quasistatic theory of line broadening. The accuracy of this approximation depends on details of the potentials, masses, and population distributions. It has been tested against fully quantum mechanical calculations and experiments for only a few cases of bound–free and free–free transitions.[5–9] Part of our purpose here is to study its range of validity for bound–bound spectra, particularly in a satellite or head of heads region. Comparisons are

made in Sec. II with the CFCP predictions for the over-all band shape and in Sec. IV with a semiclassical satellite-shape theory.[11] In Sec. III, a calculated Na$_2$ $A-X$ band fluorescence spectrum, with excitation proportional to Franck–Condon factors, is calculated and compared to measurements in an electrical discharge.[1] Also, thermal emission spectra calculated at different temperatures are compared to each other as well as to fluorescence measured by us, which comes from a nonthermal excited state formed mainly by the atom-molecule excitation transfer process, Na$(3p)$+Na$_2(X\,^1\Sigma_g)$ → Na$_2(A\,^1\Sigma_u)$+Na$(3s)$.

II. ABSORPTION AND STIMULATED EMISSION CROSS SECTIONS

A. Classical equations

In the quasistatic approximation, the classical absorption and stimulated emission cross sections for X- and A-state molecules are given respectively by[4]

$$\sigma_{ab}^{cl}=\frac{A_\nu c^2}{8\pi\nu^2}\frac{g_A}{g_X}\frac{4\pi R^2}{d\nu/dR}\frac{1}{Z_X^{cl}}\exp\left(-\frac{V_X[R(\nu)]}{kT}\right)\quad(1)$$

and

$$\sigma_{se}^{cl}=\frac{A_\nu c^2}{8\pi\nu^2}\frac{4\pi R^2}{d\nu/dR}\frac{1}{Z_A^{cl}}\exp\left(-\frac{V_A[R(\nu)]}{kT}\right),\quad(2)$$

where $V_X(R)$ and $V_A(R)$ are the adiabatic potentials for the ground and excited states as a function of internuclear distance R. The function $R=R(\nu)$ (not necessarily single-valued) defines those points at which the radiative transition at frequency ν occurs, according to the classical Franck–Condon principle

$$h\nu = V_A[R(\nu)] - V_X[R(\nu)].\quad(3)$$

The classical transition probability A_ν in (1) and (2) is identified with the quantum mechanical $A-X$ transition probability given by[12]

$$A_\nu=\frac{64\pi^4}{3}\frac{\nu^3}{hc^3}g_X D^2,\quad(4)$$

where g_X and g_A are the degeneracy factors of the X and A states (both equal to 1), D is the electronic transition dipole moment, which would normally be evaluated at $R(\nu)$ but here is taken to be independent of R for reasons discussed below, Z_X^{cl} and Z_A^{cl} are the vibration–rotation partition functions for the bounded X and A states, which have a classical form[4]

$$Z_{X,A}^{cl}=\int_0^\infty d^3R\Gamma\left(\frac{3}{2},-\frac{V_{X,A}(R)}{kT}\right)\exp\left(-\frac{V_{X,A}(R)}{kT}\right),\quad(5)$$

where, for $D_e/kT\gg1$ (D_e is the well depth), the normalized incomplete gamma function $\Gamma(\frac{3}{2},-V/kT)$ can be replaced by unity.

The assumption of a transition moment D independent of R is used above to simplify the calculation. Experiment[13] and recent calculations[14] have shown that the variation of D with R is small in the $B-X$ band of Na$_2$. For the $A-X$ system, calculations[14] and lifetime measurements[15] indicate that D varies by ~20% between 2.5 and 6 Å. This would have a minor and equal effect on

the classical and quantum mechanical calculations and would not affect their comparison and the test of the quasistatic approximation.

The value of the electronic transition moment used in the present calculation is 10.0 D for Na$_2$ (corresponding to the measured[15] and calculated[14] lifetime of 12 nsec for the low vibration levels of the A state), and 6.58 D for Li$_2$ (corresponding to a calculated lifetime[16] of 32.6 nsec at $\langle\lambda^3\rangle=4.43\times10^{-13}$ cm^3).

The stimulated emission cross section can be obtained from the absorption cross section at the same temperature according to

$$\sigma_{se}=\sigma_{ab}\frac{Z_X g_X}{Z_A g_A}\exp\left(-\frac{h\nu}{kT}\right).\quad(6)$$

A classical satellite occurs at frequency ν_s when there is an extremum in the potential difference curve between excited and ground state, $(d\nu/dR)_{\nu_s}=0$ in Eq. (1). The classical spectrum, as given by Eq. (1), diverges at the satellite and has no intensity beyond ν_s, due to the assumption of conservation of nuclear momenta in CFCP.

B. Quantum mechanical equations

In the quantum mechanical calculation, the transition $(v'',J'')\to(v',J')$ occurs at

$$h\nu=E'(v',J')-E''(v'',J''),$$

with an intensity proportional to[12]

$$I_{v'J'}^{v''J''}=\nu\exp(-E''/kT)\,\omega_{J''}S_{J'J''}\langle v'|v''\rangle^2 D^2,\quad(7)$$

where $S_{J'J''}$ is the Hönl–London factor, equal to $\frac{1}{2}(J'+J''+1)$ with $J'=J''\pm1$ for a $^1\Sigma-^1\Sigma$ transition, $\langle v'|v''\rangle^2$ is the Franck–Condon factor, assumed to be independent of J, D is the electronic transition moment, and $\omega_{J''}$ is a statistical factor due to nuclear spin:

$$\omega_J=\begin{cases}I/(2I+1)&\text{for even }J''\\(I+1)/(2I+1)&\text{for odd }J'',\end{cases}\quad(8)$$

I being the half-integral nuclear spin of Na^{23} and Li^7. The absorption cross section, averaged over an interval of $\Delta\nu$, is

$$\sigma_{ab}^{QM}=\frac{1}{\Delta\nu}\frac{8\pi^3 g_A}{3hcZ_R Z_v}\sum_{J'J''v'v''}^{\Delta\nu}I_{v'J'}^{v''J''},\quad(9)$$

where the summation is over all transitions $(v'',J'')\to(v',J')$ that fall within the interval $\nu\to\nu+\Delta\nu$. Z_R and Z_v are the rotation and vibration partition functions,

$$Z_R\simeq\sum_{J''}(2J''+1)\,\omega_{J''}\exp\left(-\frac{hcB_e''J''(J''+1)}{kT}\right)$$

$$\simeq\frac{kT}{hcB_e''},\quad(10)$$

and

$$Z_v\simeq\sum_v\exp\left(-\frac{hc\omega_e(v+1/2)}{kT}\right).\quad(11)$$

C. Vibration band continuum approximation

In the band calculation we average the intensity of the rotation lines over an interval $\Delta\nu$ smaller than the typi-
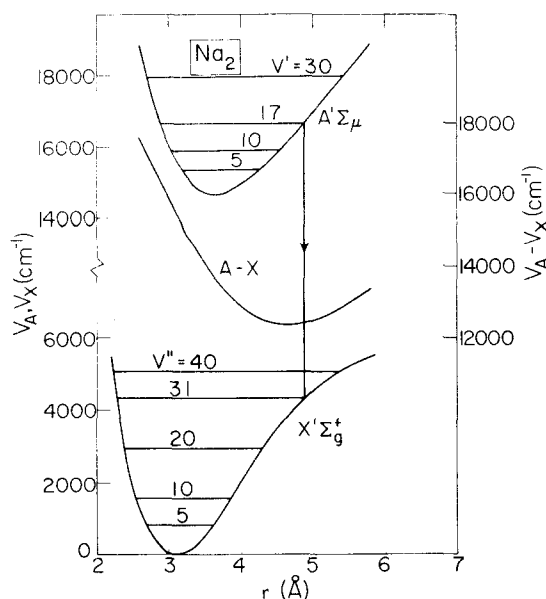
FIG. 1. Adiabatic potentials of the $A\,^1\Sigma_u$ and $X\,^1\Sigma_g$ states of Na_2. The quantum mechanical head of bands is the (v',v'') = (17, 31) band at 12 405 cm^{-1}. The classical satellite is at 12 355 cm^{-1}.

cal spacing of the more intense vibration bands, $\lesssim hc\omega_e$, but larger than the typical spacing of the rotation lines, $\lesssim (2\bar{J}+1)hc\Delta B$ [where $\bar{J} \sim (kT/2hcB)^{1/2}$ is the rotation level with maximum population at temperature T, and $\Delta B = B_{v'} - B_{v''}$]. In this averaging process, the vibration–rotation lines are smoothed out and the difference in nuclear spin factor for even and odd J's can be neglected by putting $\omega_J = \frac{1}{2}$. P and R branches are also replaced with two Q branches, $J' = J'' = J$. In general, the frequency of a given rotation–vibration transition can be expressed as a sum over various molecular constants B_v, D_v, etc.[12]:

$$h\nu = E'(v',J) - E''(v'',J)$$
$$= h\nu_{v'v''} - hc\Delta B J(J+1) + hc\Delta D J^2(J+1)^2 \ldots, \quad (12)$$

where $h\nu_{v'v''} = E'(v',0) = E''(v'',0)$, and $\Delta D = D_{v'} - D_{v''}$. When the distribution is transformed from discrete rotation lines J to a continuous distribution of frequency ν, the transformation factor $|d\nu/dJ| \cong c\Delta B(2J+1)$ cancels the J dependence in the Hönl–London factor $S_{JJ} = \frac{1}{2}(J'+J''+1) \approx \frac{1}{2}(2J+1)$ and we have a continuous distribution expression for (9):

$$\sigma_{ab} = \frac{8\pi^3 g_A}{3hc Z_R Z_v} \sum_{v',v''} \left[\frac{\nu_{v'v''}}{2c\Delta B} \langle v' | v'' \rangle^2 D^2 \right.$$
$$\times \exp\left(-\frac{E''(v'',0)}{kT} \right) \Bigg]$$
$$\times \left[\frac{\nu}{\nu_{v'v''}} \exp\left(-\frac{B_{v''}(\nu_{v'v''} - \nu)}{\Delta B kT} \right) \right]. \quad (13)$$

The first bracket represents the vibration band intensity and the second bracket represents the shape of the band due to rotational populations. This band shape is essentially a simple exponential fall off from a head at $J=0$. It is shaded to the red for the alkali dimer $A-X$ bands.

Inclusion of the second order ΔD term in (13) is necessary at large v' and v'', since ΔB becomes small. The ΔD term is also important on the far side of the red satellite since the rotational parts of many vibrational bands are red-shaded into this region. Inclusion of the second order term replaces the rotational part in the bracket of Eq. (13) by $(\nu/\nu_{v'v''})[\mu(x_-) + \mu(x_+)]$, where

$$x_\pm = \frac{\Delta B \pm [\Delta B^2 + 4\Delta D(\nu_{v'v''} - \nu)]^{1/2}}{2\Delta B}$$

and

$$\mu(x) = \frac{\Delta B}{|\Delta B - 2x\Delta B|} \exp\left(-\frac{hc(B_{v''}x - D_{v''}x^2)}{kT} \right). \quad (14)$$

D. Calculation and results

The molecular constants needed in the calculation are given as Dunham coefficients in Refs. 17 and 18. Using the Rydberg–Klein–Rees (RKR) method, these coefficients generate the adiabatic potential curves for the A and X states of Na_2 and Li_2, shown in Figs. 1 and 2. Mixing with the $a\,^3\Pi_u$ state is neglected, as this perturbation only shifts a few A-state rotation lines by as much as 1 cm^{-1} and does not affect the wavelength-averaged band intensities.[17] The Franck–Condon factors for $J = 0$ are then calculated using the RKR wavefunctions. Dependence of strong Franck–Condon factors on J is small, so it is neglected.

At the temperatures we consider, the thermal absorption and emission spectra are dominated by bound–bound transitions, except near the free Na and Li transition wavelengths (589 and 670 nm). For Na_2, the A and X states have well depths of ~8200 and ~5900 cm^{-1}, respectively, compared to a value of kT at 800 K (P_{Na} = 6.5 Torr) of 555 cm^{-1}. For Li_2, the A and X state well depths are 9500 cm^{-1} and 8600 cm^{-1} compared to kT at 1020 K (P_{Li} = 1 Torr) of 708 cm^{-1}.

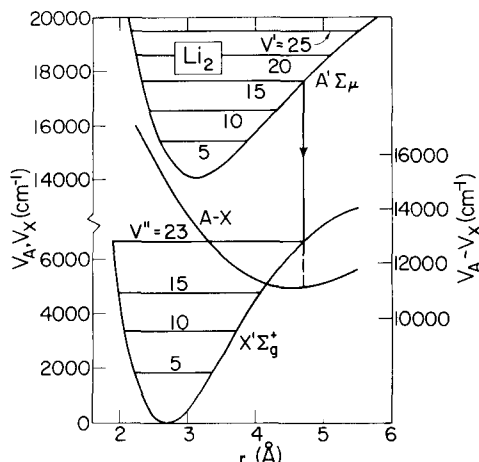Some of the vibrational band intensities [the term in the first bracket of (13)] for Na_2 are plotted in Fig. 3,

FIG. 2. Adiabatic potentials of the $A\,^1\Sigma_u$ and $X\,^1\Sigma_g$ states of Li_2. The quantum mechanical head of bands is the (v',v'') = (15, 23) band at 10 980 cm^{-1}. The classical satellite is at 10 952 cm^{-1}.
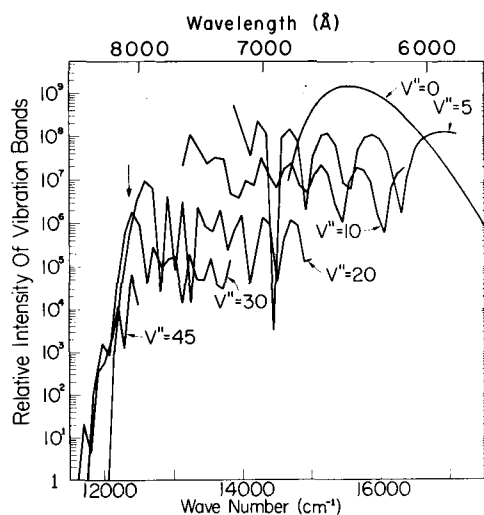
FIG. 3. Relative intensities of some vibration bands of Na$_2$ vs band-head frequencies. Bands with the same v'' are connected, by straight lines, e.g., for $v'' = 5$ and 10, v' ranges from 0 on the left to 30 on the right. For larger v'', $v' = 30$ on the right but the smaller v' values fall below the axis. The arrow indicates the classical satellite position.

FIG. 5. Absorption and stimulated emission cross sections of the $A-X$ band of Li$_2$ at 1020 K. For labeling of curves, see Fig. 4 caption. Three dominant vibration bands (v', v'') at 13 500 cm^{-1} are shown to scale with respect to curve C.

for $v' = 0-30$ and some selected values of v''. The absorption and stimulated emission coefficients calculated by the three different methods are shown in Fig. 4 for Na$_2$ and Fig. 5 for Li$_2$. Note that the overall absorption band shape in Fig. 4 approximately follows the upper envelope in Fig. 3, which becomes smoothed by the addition of the other v'' bands.

The line summation calculation involves computing according to (9) the intensities of ~ 200 000 vibration–rotation transition lines in the case of Na$_2$ (100 000 in the case of Li$_2$). These lines were ordered according to

their wave numbers and grouped into channels of width $\Delta \nu$ which was taken to be 5 cm^{-1} in Fig. 4 and 8 cm^{-1} in Fig. 5. Both the "line summation" and "continuum band approximation" calculations have been folded with a Lorentzian line profile function of full width equal to two channels, thus rounding off the sharpness of the edges.

The effect of grouping the calculated line intensities into these large $\Delta \nu$ channels is demonstrated in Fig. 6. This figure shows a blowup of the 14 450–14 600 cm^{-1} region of the curve labeled F in Fig. 4. In this blowup, the individual vibration–rotation transition lines are plotted before they are averaged. This portion of the $A-X$ band is relatively simple because of the dominance
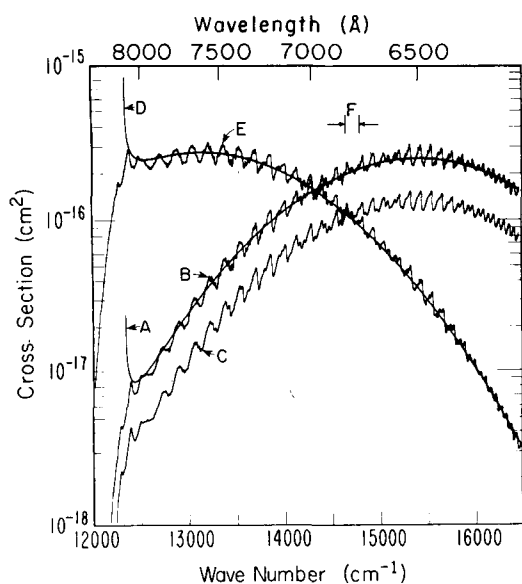

FIG. 4. Absorption and stimulated emission cross sections of the $A-X$ band of Na$_2$ at 800 K. The absorption curves are A: classical, B: line calculation, and C: band calculation displaced by a factor of 2. The emission curves are D: classical and E: line calculation. F is the portion shown in Fig. 6.
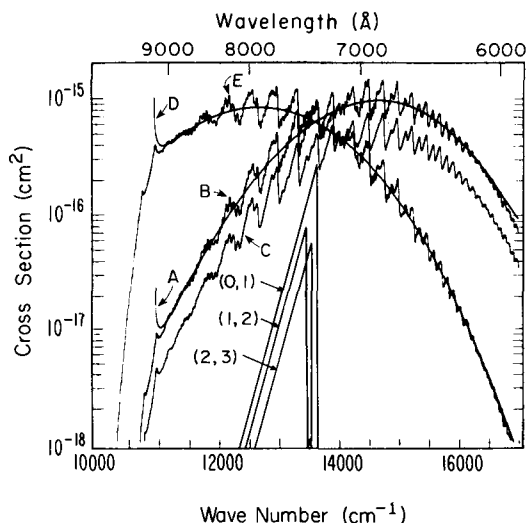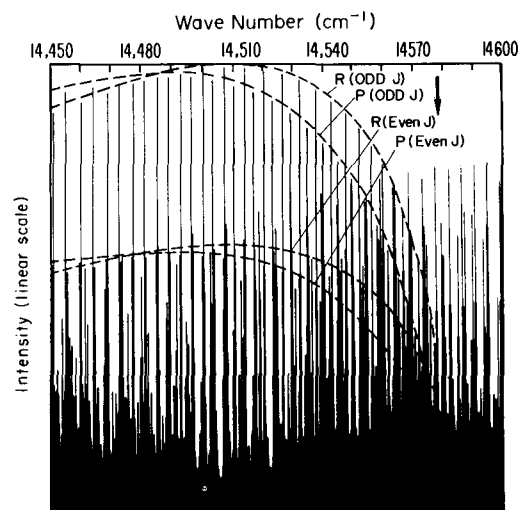

FIG. 6. Vibration–rotation absorption lines in the $A-X$ band of Na$_2$ at 14 500 cm^{-1}. The four envelop lines for R and P branches and even and odd J'' values of the $(v', v'') = (2, 2)$ band are drawn. The arrow indicates the band-head position. The absorption lines peak at $J \sim 43$. After wavelength averaging, the vibration band has a maximum at the band head.
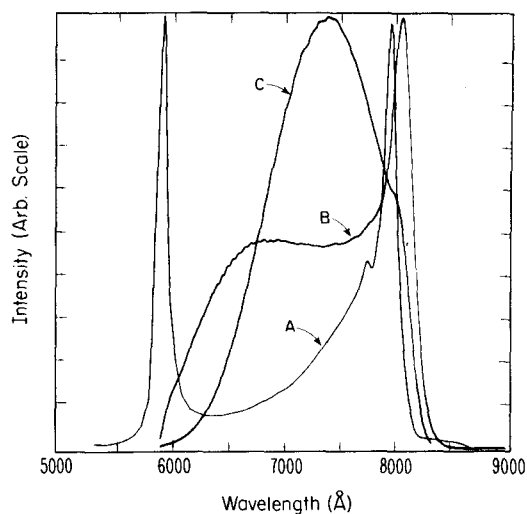
FIG. 7. Comparison of measurement from Ref. 1 (A) with calculations of an electron excited fluorescence (B) and a thermal emission (C). All curves are at 709 K. The calculated curves have been folded with a triangular function of 200 cm^{-1} width, representing the experimental resolution.

of the $(v', v'') = (2, 2)$ band, yet the unaveraged line spectrum in Fig. 6 shows no resemblance to the $\Delta\nu$ averaged spectrum in Fig. 4. It is necessary to average over at least $\Delta\nu = 3$ cm^{-1} to obtain a simple intensity pattern as in Fig. 4.

Several approximations have been made in calculating these band intensities, and will now be discussed. In the line–summation calculation we have neglected vibrational bands with small Franck–Condon factors, such that the v', v'' band intensity at λ is less than 10^{-2} of the average $A-X$ band intensity at λ. A test calculation using the "continuum band approximation" indicated that the net contribution of all of these weak bands to the final k_ν is less than 2%.

The effect of truncating v' and v'' is negligible in the centers of the bands, but can affect the intensity at $k < k_{\text{satellite}}$ and at $k > 16\,000$ cm^{-1}. The truncation of v' at 30 for Na$_2$ and Li$_2$ omits some intensity at $k > 16\,000$ cm^{-1} for both cases. This can be seen in Figs. 4 and 5, where the classical calculation, which effectively includes all v', rises above the vibrational band calculations. It can also be seen in Fig. 3 that extending the $v'' = 5$ and 10 lines to larger v' would yield a noticeable increase in intensity at $k > 16\,000$ cm^{-1}. The contributions to the Na$_2$ satellite region (12 200–12 700 cm^{-1}) are expected to be strongest for v' and v'' levels, with turning points near 4.7 Å in Fig. 1, i.e., $v' \cong 10$ and $v'' \cong 25$. As v'' increases past 30 the contributions decrease rapidly, as can be seen in Fig. 3. The inclusion of v'' up to 45 for Na$_2$ is estimated to be sufficient to yield the satellite shape in the $> 12\,200$ cm^{-1} region with better than 10% accuracy. The inclusion of Li$_2$ levels up to $v' = 30$, $v'' = 3$ is expected to have a similar accuracy (compare Figs. 1 and 2).

Rotational levels up to $J = 150$ have been included in the line summation calculation. The band intensity contribution of the remaining lines to the band intensity can

be seen by comparing the continuum at the cutoff of $J = 150$ to that at the band head ($J = 0$). This is an intensity factor of $\exp[-hcB''J(J+1)/kT] \sim 2 \times 10^{-3}$ in the case of Na$_2$, and smaller in the case of Li$_2$. To first order this cutoff occurs about $\Delta BJ(J+1) \sim 1000$ cm^{-1} in the case of Na$_2$, and ~ 3800 cm^{-1} in the case of Li$_2$, to the red of the vibration band head. Except at $\nu \ll \nu_{\text{satellite}}$, where the $A-X$ band is very weak, such a cutoff does not affect the overall spectral intensity.

For almost all vibrational bands, $\Delta B = B_{v''} - B_{v'} > 0$, producing a shading to the red side. The long–wavelength side of the satellite is sensitive to the higher order rotational constants, which determine how the tails of the vibrational bands roll off. Dependence of the Franck–Condon factors on J may also be important in this region but have not been included here. The second order $\Delta D_v J^2 (J+1)^2$ term in rotation energy [Eq. (13)] causes the tail of the vibration band to turn around at a value of $J \cong (\Delta B_v/2\Delta D_v)^{1/2}$. Thus Eq. (14) instead of the more approximate Eq. (13) produces a rolloff for $\nu \ll \nu_s$ in much better agreement with the "line summation" calculation (compare curves of "line summation" and "continuum band approximation" calculations for Na$_2$ in Fig. 9). However, for $\nu > \nu_s$ Eq. (13) is entirely adequate and has been used to obtain the intensities in Figs. 4 and 5.

III. COMPARISON WITH SOME MEASURED SPECTRA

One example of a nonthermal spectrum is electron or white-light excited fluorescence emission in a system like Na$_2$. For simplicity in calculation and lack of information on the electron excitation of the Na$_2$ $A-X$ system, we assume the excitation to be proportional to Franck–Condon factors and that the change in rotation quantum number is negligible, $J' \simeq J''$. The validity of these assumptions is uncertain for low or medium energy electrons (i.e., below the Born approximation regime) especially near threshold when quasimolecular ion resonances may be present.

Briefly, the calculation gives an excited A-state vibration level population of

$$N_{v'} \propto \sum_{v''} \langle v' | v'' \rangle^2 \exp\left(- \frac{E''(v'', 0)}{kT}\right),$$

when a Boltzmann distribution is assumed in the ground X state. An A-state rotational population distribution $(2J+1)\exp[-B_{v'''}J(J+1)/kT]$, corresponding to a rotational temperature $T_R = (B_{v'}/B_{v''})\,T$, results from the $\Delta J = 0$ assumption. In the absence of relaxation in the excited state the fluorescence photon intensity is then given by an expression similar to (13) but with these modified population factors for v', J':

$$I \propto \sum_{v'v''} \nu^3 \langle v' | v'' \rangle^2 N_{v'} \exp\left(- \frac{B_{v''}(\nu_{v'v''} - \nu)}{\Delta BkT}\right). \quad (15)$$

To simplify the actual calculation, a typical constant value B' is usual for $B_{v'}$ and B'' for $B_{v''}$. In Fig. 7, the calculated spectrum, after being folded with a triangular function of full width 200 cm^{-1}, is compared to the measured emission spectrum of Sorokin $et\,al.$[1] from a 25 mA sodium discharge operated at 709 K and 25 mA in a 1-m heat pipe. The experimental curve in Fig. 7
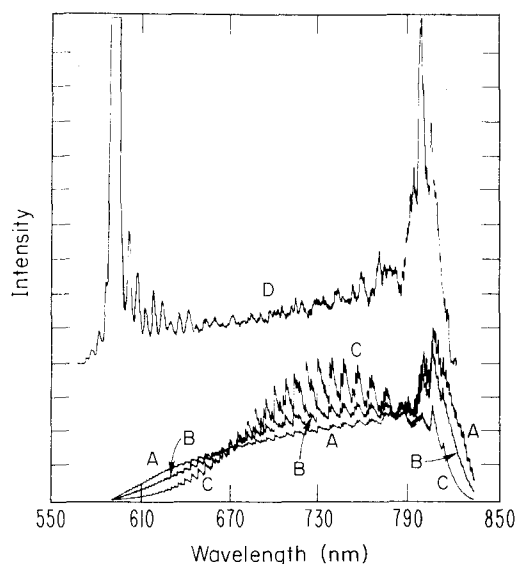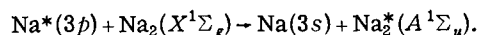
FIG. 8. Comparison of a nonthermal distribution spectrum (D) of Na₂ $A\,^1E$ state formed by atomic–molecule excitation transfer with thermal emission spectra at 3000 K (A), 1500 K (B), and 800 K (C). The curves are normalized to have equal area in the $A-X$ band.

is only approximate due to difficulties in reproducing the curve from the original paper. The accuracy of the wavelength scale of the prism monochromator used in the measurement is not known to us. Discrepancy in the central portion of the spectrum could be due to absorption of fluorescence radiation by the X-state low lying vibration levels, which have absorption bands centered about 14 500 cm⁻¹. Such a self-reversal is probable in the molecular band because the fluorescence comes from a long (1 m) positive column viewed through the end of the heat pipe.

In Fig. 8, spontaneous emission spectra for a Boltzmann distribution of excited Na₂ $A\,^1\Sigma$ state at 800, 1500, and 3000 K is plotted and compared with the fluorescence spectrum we measured due to excited $A\,^1\Sigma$ state formed by an atom–molecule excitation transfer process at 743 K:

$$\mathrm{Na^*}(3p) + \mathrm{Na_2}(X^1\Sigma_g) \rightarrow \mathrm{Na}(3s) + \mathrm{Na_2^*}(A\,^1\Sigma_u).$$

The prominence of the red satellite in both experimental curves compared to thermal spectra at different temperatures indicates that the excited state distribution corresponds to a very high effective temperature. The presence of strong bands near the atomic line in the experimental curve (D) of Fig. 8 shows that high vibrational levels close to the dissociation limit are populated. The similarity of the two experimental curves in Figs. 7 and 8 suggests that the process of atom–molecule excitation transfer may also be important in the curve of Fig. 7.

IV. SATELLITE SHAPE

The three thermal emission curves in Fig. 8 show that as temperature increases, the satellite becomes more prominent as well as broadens out to the red side.

Another comparison of satellite shape is with Sando and Wormhoudt's (SW) semiclassical theory[11] as applied to a bound–bound system. In the approximation of parabolic potential differences near the satellite frequency, the unified Franck–Condon theory of Ref. 19 reduces to the SW theory, so we do not make a separate comparison to Ref. 19. As pointed out in the Appendix of Ref. 20, an extension of Sando's theory to a bound–bound system involves the universal satellite function $T(u, \infty)$ tabulated in Ref. 9,

$$\sigma_{ab} \propto \nu\, T(u, \infty).$$

The reduced frequency unit is

$$u = (\mu / \hbar^2 k T \Delta v'')^{1/3}\, h(\nu_s - \nu), \tag{16}$$

where μ is the reduced mass of the dimer system, ν_s the classical satellite frequency, and $\Delta v''$ the curvature of the difference potential at the satellite. In Fig. 9, the calculated absorption spectrum σ_{ab}/ν of Na₂ and Li₂ is compared to $T(u, \infty)$. The straight line G drawn in Fig. 9 represents an asymptotic exponent of $12^{1/3}\,u \simeq 2.29\,u$ of $T(u, \infty)$ for large positive u, corresponding to $\nu \ll \nu_s$. The rolloffs of the satellite tails for Li₂ versus Na₂ are similar, indicating that the reduction to the dimensionless parameter u is appropriate. The rate of decrease beyond the satellite predicted by SW theory also appears to be reasonable, but the magnitude differs considerably. The difference on the near side of the satellite is due to the parabolic approximation in the SW theory, and can be removed by the use of the Ref. 19 theory.
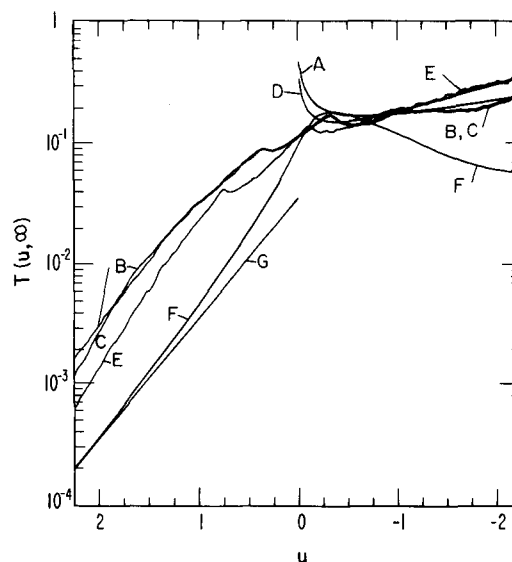

FIG. 9. Comparison of calculated satellite shapes with Sando and Wormhoudt's semiclassical theory. u is a reduced unit of frequency, with $u = 0$ at the classical satellite (ν_s). A: Na₂ classical calculations, B: Na₂ line calculation, C: Na₂ band calculation, D: Li₂ classical calculation, E: Li₂ line calculation, F: Sando and Wormhoudt's satellite function $T(u, \infty)$, G: asymptotic exponent of $T(u, \infty)$ at large u. The calculated band intensities have been approximately normalized to curve F at $u = 0$. For the $A-X$ band of Na₂, one u unit is ~155 cm⁻¹ and for Li₂, ~246 cm⁻¹.

V. CONCLUSIONS

We have shown that the classical spectrum based on the quasistatic or classical Franck–Condon approximation describes the main part of the molecular band rather well (see Figs. 4 and 5), except for undulations which are dependent on the temperature and mass of the molecule. For Na_2 and Li_2 at temperatures corresponding to a few Torr of pressure, the undulation is ~ 20–50%. A continuum distribution for the vibration bands greatly simplifies the quantum mechanical calculation and closely approximates the results of the fully quantized calculation. Both the Na_2 and Li_2 satellite intensities roll off at roughly the same rate when expressed in terms of the reduced frequency unit u in Eq. (16), agreeing qualitatively, but not quantitatively, with the semiclassical calculation of Ref. 11 (see Fig. 9). However there are undulations in the quantum mechanical calculation extending beyond the satellite position that are not present in the semiclassical theory, and there is a discrepancy in total intensity. Comparison of calculated thermal emission spectra at different temperatures with the measured spectrum of Fig. 8 suggests an excited state "effective" temperature that is very high or even inverted (see Sec. III). Molecular constants of higher order than those presently known are required for an adequate comparison in the 590–620 nm region. Also, the effect on a high temperature spectrum of $A\,^1\Sigma$ and $a\,^3\Pi$ state mixing should be examined.

†Staff Member, Laboratory Astrophysics Division, National Bureau of Standards.

[1] P. P. Sorokin and J. R. Lankard, J. Chem. Phys. 55, 3810 (1971).

[2] J. M. Anderson, J. Appl. Phys. 46, 1531 (1975); R. E. Kinsinger, 27th Annual Gaseous Electronic Conf., Houston, Texas, 1974 (unpublished).

[3] A. V. Phelps, "Tunable Gas Lasers Utilizing Ground State Dissociation," JILA Report 110, Univ. of Colorado, 1972.

[4] G. York and A. Gallagher, "High Power Gas Lasers Based on Alkali-Dimer A–X Band Radiation," JILA Report 114, Univ. of Colorado, 1974.

[5] F. H. Mies, J. Chem. Phys. 48, 482 (1968); R. O. Doyle, J. Quant. Spectrosc. Radiat. Transfer 8, 1555 (1968); A. Dalgarno, G. Herzberg, and T. L. Stephens, Astrophys. J. Lett. 162, 49 (1970); T. L. Stephens and A. Dalgarno, J. Quant. Spectrosc. Radiat. Transfer 12, 569 (1972).

[6] G. H. Dunn, Phys. Rev. 172, 1 (1968).

[7] F. H. Mies and A. L. Smith, J. Chem. Phys. 45, 994 (1966).

[8] K. M. Sando and A. Dalgarno, Mol. Phys. 20, 103 (1971).

[9] C. G. Carrington, D. Drummond, A. Gallagher, and A. V. Phelps, Chem. Phys. Lett. 22, 511 (1973).

[10] R. L. LeRoy, R. G. McDonald, and G. Burns, J. Chem. Phys. 65, 1485 (1976).

[11] K. M. Sando and J. C. Wormhoudt, Phys. Rev. A 7, 1889 (1973).

[12] G. Herzberg, *Molecular Spectra and Molecular Structure*, 2nd ed. (Van Nostrand, New York, 1950), Vol. I.

[13] M. M. Hessel, E. W. Smith, and R. E. Drullinger, Phys. Rev. Lett. 33, 1251 (1974).

[14] W. J. Stevens, M. M. Hessel, P. J. Bertoncini, and A. C. Wahl, J. Chem. Phys. (in press).

[15] D. Kleppner (private communication).

[16] W. J. Tango, Ph. D. Dissertation, Univ. of Colorado, Boulder, CO, 1969. The Li_2 and Na_2 A-state lifetimes calculated here should be divided by 2, according to Ref. 14.

[17] P. Kusch and M. M. Hessel, J. Chem. Phys. 63, 4087 (1975). The A-state constants have been revised, see M. M. Hessel and P. Kusch, in Abstracts, First Symposium on Molecular Spectroscopy, Columbus, Ohio, 1976; W. Demtroder, M. McClintock, and R. N. Zare, J. Chem. Phys. 51, 5495 (1969).

[18] D. Hsu, Ph. D. Dissertation, Fordham Univ., New York, 1975, unpublished.

[19] J. Szudy and W. E. Baylis, J. Quant. Spectrosc. Radiat. Transfer 15, 641 (1975).

[20] C. G. Carrington and A. Gallagher, Phys. Rev. A 10, 1464 (1974).